Available online at www.sciencedirect.com
SCIENCE DIRECT
Polymer 47 (2006) 3609–3615
polymer
www.elsevier.com/locate/polymer

Effects of silicalite-1 nanoparticles on rheological and physical properties of HDPE

Dong Wook Chae [a], Kwang Jin Kim [b], Byoung Chul Kim [a,*]

[a] Division of Applied Chemical and Bio Engineering, Hanyang University, 17 Haengdang, Seongdong, Seoul 133-791, South Korea
[b] Korea Institute of Ceramic Engineering and Technology, 233-5, Gasan, Guemcheon, Seoul 153-801, South Korea

Received 21 July 2005; received in revised form 3 January 2006; accepted 17 March 2006

Abstract

The addition of silicalite-1 nanoparticles (0.2–20 wt%) increased slightly the crystallization temperature of HDPE with silicalite-1 content, at 20 wt% loading by ca. 2.5 °C, but it had little effect on the melting temperature. The nanocomposites displayed a little higher onset degradation temperature than pure polymer by 7–11 °C. The WAXD profiles showed that the intensity of diffraction peaks for HDPE was decreased with increasing silicalite-1 content from 5 wt% but that the peak position of every crystal plane did not shift in the presence of silicalite-1 nanoparticles. The incorporation of the nanoparticles increased the melt viscosity of HDPE with silicalite-1 content. It also increased both storage (G') and loss modulus (G''). In the so-called Cole–Cole plot, pure HDPE showed a single master curve whose slope was 1.37, while the nanocomposites with 10 and 20 wt% silicalite-1 exhibited the inflection in the low frequency range before which the slopes were 1.22 and 1.02, respectively. Much more accelerated crystallization behavior under shear was observed with silicalite-1 content at the isothermal crystallization temperature of 125 °C than at 120 °C.

Keywords: High density polyethylene; Silicalite-1; Nanocomposites

1. Introduction

Recently, organic–inorganic nanocomposites are in the spotlight as a promising class of materials because of their advantages and unique properties synergistically derived from nano-scale structure. These nanocomposites exhibit improved mechanical properties, low thermal expansion coefficient, high barrier properties, flame retardancy, and swelling resistance [1–5]. Further, these benefits can be achieved even at very low concentration in comparison to conventional polymer composites. Sometimes, they possess the transparent properties presumably attributable to the nano-scale phenomena of the hybrids [6].

Inorganic nanoparticle can be manufactured in a mass and its application to the organic material made commercial success in nylon 6 [7]. However, the control of the structures and properties of nanocomposites is limited only by our current understanding of their characteristic features. This seems to originate from unusually large specific surface area of nanoparticles. Thus, many studies on the preparation, structures, and physical properties of polymer/inorganic nanocomposites have been extensively made; however, relatively limited work has been carried out on the rheological behaviors, which are related to the distortion or deformation of polymer chain. In addition, the real polymer processing involves very complicated deformation histories, which may affect the nucleation and crystallization behavior of polymers. Thus, understanding the nucleation and crystallization processes under shear is significant because they offer a critical clue to optimize the processing of molding compounds.

High density polyethylene (HDPE) is among the most widely used polyolefin polymers because of its high strength, cheap cost, excellent processability, and high chemical resistance. Silicalite-1 is the stable aluminum-free form of MFI type zeolites, which was firstly introduced by Flanigen et al. as a new hydrophobic but organophilic polymorph of silica [8]. Introduction of silicalite-1 nanoparticles is expected to provide functionalities to the polymers, such as separation and adhesion capacity of noxious organic matter or ion.

There are several general ways of dispersing nanofillers in polymers such as direct mixing either in melt [9,10] or solution [11] and in situ polymerization [12,13] in the presence of

* Corresponding author. Tel.: +82 2 2220 0494; fax: +82 2 2297 4941.
E-mail address: bckim@hanyang.ac.kr (B.C. Kim).

0032-3861/$ - see front matter © 2006 Elsevier Ltd. All rights reserved.
doi:10.1016/j.polymer.2006.03.053

the nanoparticles. However, for most technologically important polymers, solution mixing and in situ polymerization are limited since neither a suitable monomer nor a compatible solvent is always available. Thus, melt compounding is a promising approach to fabricate hybrid plastic materials because of its low cost, high productivity, and compatibility with conventional polymer processing techniques [14]. In this study, HDPE/silicalite-1 nanocomposites were prepared by melt mixing and their physical properties were discussed including thermal properties, rheology, morphology, and crystallization behavior under shear.

2. Experimental

2.1. Materials and sample preparation

Tetrapropylammonium hydroxide (TPAOH, 1.0 M aqueous, Aldrich), sodium hydroxide (NaOH, Yakuri), and sodium dihydrogenphosphate (NaH_2PO_4, Aldrich) were used as starting materials and fumed silica (Cab-O-Sil M-5) was used for silica source. Synthesis of silicalite-1 was made from a clear homogeneous solution with a molar composition of $1TPAOH:3SiO_2:0.2NaH_2PO_4:70H_2O$. The solution was hydrolyzed at room temperature for 24 h with vigorous stirring. Crystallization was then carried out at 100 °C after predetermined time (12 h) at 60 °C, using a hydrothermal system. After crystallization, the solid products were recovered by centrifugation, washed thoroughly with deionized water, dried at 80 °C, and calcined in the air at 550 °C for 10 h. The silicalite-1 nanoparticles thus prepared were round-shaped ones and their size ranged from 100 to 200 nm, as shown in Fig. 1. High density polyethylene (HDPE) with a melt flow index of 36 g/10 min was purchased from Aldrich, Inc. The HDPE was vacuum dried at 80 °C for 24 h prior to melt mixing with the silicalite-1 nanoparticles. The HDPE and silicalite-1 nanoparticles were dry-mixed via tumbling in a bottle. Compounding of the premixture was then done using an internal mixer (Haake Rheomix 600) at 170 °C at a rotor speed of 60 rpm for 3 min. The loading levels (X) of the nanocomposites were 0.2, 1, 5, 10, and 20 wt%, and they were coded HDPE-X.

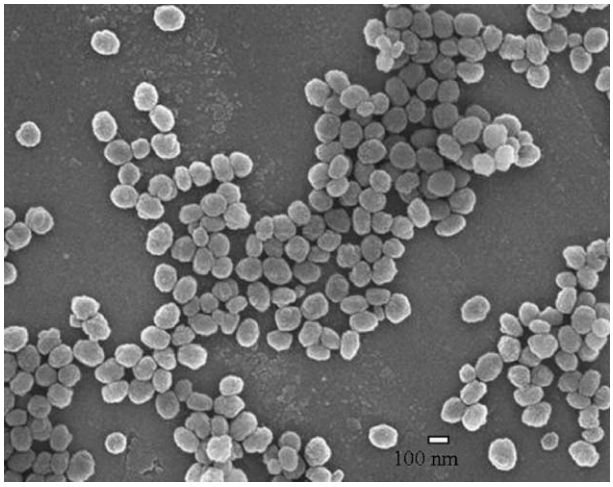

Fig. 1. FESEM image of silicalite-1 nanoparticles prepared from two stage synthesis.

2.2. Measurement of physical properties

The morphology of the nanocomposites was examined using a field emission scanning electron microscope (FESEM; JEOL, JSM-6340F). FESEM specimens were prepared in the films with thickness of ca. 0.5 mm by using a standard hot press. The film surfaces were then sputter-coated with a thin gold layer to avoid charging.

Differential scanning calorimetry (DSC) measurements were performed on a TA Instruments DSC 2010 in a nitrogen atmosphere. The samples were held at 170 °C for 5 min to eliminate the thermal history, and then cooled to 30 °C at 10 °C/min, and finally heated again to 170 °C at the same rate. Thermal gravimetric analysis (TGA) was carried out using SDT2960 (TA Instruments, Dupont). The TGA scans were recorded from 30 to 800 °C at 10 °C/min in a nitrogen atmosphere.

The rheological properties were measured with an advanced rheometric expansion system (ARES; Rheometric Scientific, Inc.). Parallel plate geometry with a diameter of 25 mm was employed. The plate gap and strain level were 1 mm and 10%, respectively. The specimen was melted at 150 °C between the parallel plates and kept for 3 min at the temperature in nitrogen atmosphere to remove the residual stress. Frequency sweep measurement was conducted over the angular frequency range of 0.05–500 rad/s. The crystallization behavior under shear was examined in time sweep mode at an angular frequency of 5 rad/s. The temperature was raised to 150 °C and held for 3 min, and then lowered to the desired crystallization temperatures of 120 and 125 °C.

The crystal structure of silicalite-1 reinforced HDPE was determined by wide angle X-ray diffraction (WAXD), using a Rigaku Denki (D/MAX-2000) with nickel filtered Cu K_α radiation of 40 kV and 100 mA. Scanning was carried out on the equator in the 2θ angle ranging from 5 to 30° at a scan speed of 5°/min.

3. Results and discussion

The dispersion state of HDPE/silicalite-1 nanocomposites is determined by FESEM. Fig. 2 exhibits the surface morphology of the HDPE nanocomposites with 5 wt% silicalite-1. The silicalite-1 nanoparticles are finely dispersed in the HDPE matrix without large agglomerate.

The DSC cooling and the second heating scan of HDPE and HDPE/silicalite-1 nanocomposites are shown in Fig. 3(a) and (b), respectively. Introducing silicalite-1 nanoparticles increases slightly the crystallization temperature (T_c) by ca. 2.5 °C when comparing HDPE-20 with pure HDPE. In addition, it increases the heat of crystallization (ΔH_c) of HDPE from 219.5 to 237.8 J/g with silicalite-1 content. These results suggest that the nanoparticles play a role of nucleating agent for HDPE and thereby promote crystallization through

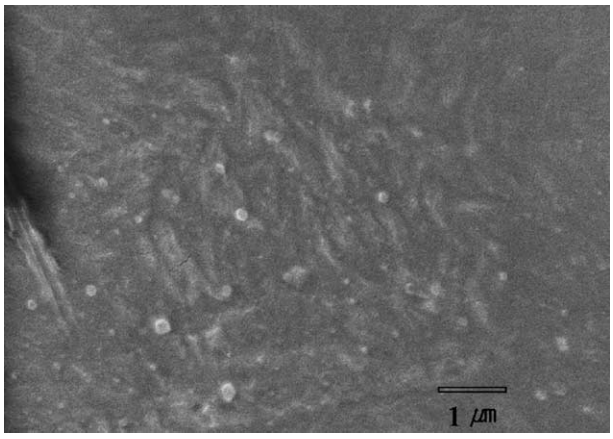

Fig. 2. FESEM images of HDPE nanocomposites with 5 wt% silicalite-1.

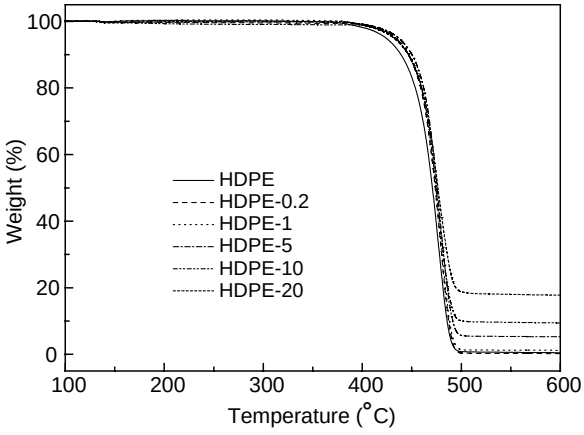

Fig. 4. TGA thermograms of HDPE and HDPE/silicalite-1 nanocomposites.

heterogeneous nucleation. However, as shown in Fig. 3(b), the introduction of silicalite-1 nanoparticles has little influence on the melting temperature of HDPE but it increases the heat of fusion (ΔH_m) from 225 to 241 g/J.

The thermal degradation profiles of HDPE and HDPE/silicalite-1 nanocomposites exhibit that most of the degradation events occur between 365 and 520 °C in Fig. 4. Thermal stability of HDPE is increased with silicalite-1 content. The nanocomposites degrade over a much narrower temperature range than the pure polymer because the onset point of degradation shifts to higher temperature. When considering the degradation temperature ($T_{0.1}$), required for 10% weight loss, the nanocomposites display a little higher $T_{0.1}$ than pure polymer by 7–11 °C. This suggests that the silicalite-1 nanoparticles in the polymer matrix play a role in preventing the permeation of the heat and out-diffusion of polymeric material.

WAXD profiles of HDPE and its nanocomposites with silicalite-1 are given in Fig. 5. Within the given range of scattering angles, there are five local maxima at 2θ values of approximately 7.8, 8.7, 21.3, 22.9, and 23.7°. The diffraction peaks at 7.8, 8.7, and 22.9° correspond to the (101), (200), and (501) reflections of silicalite-1, respectively, and 21.3 and 23.7°, (110) and (200) those of HDPE, respectively. The diffraction peaks associated with silicalite-1 are not observed up to 1 wt% loading, after which the peaks get more prominent with increasing the silicalite-1 content. The intensity of diffraction peaks for HDPE decreases with increasing silicalite-1 content from 5 wt%. This indicates that the amount ratio of HDPE to

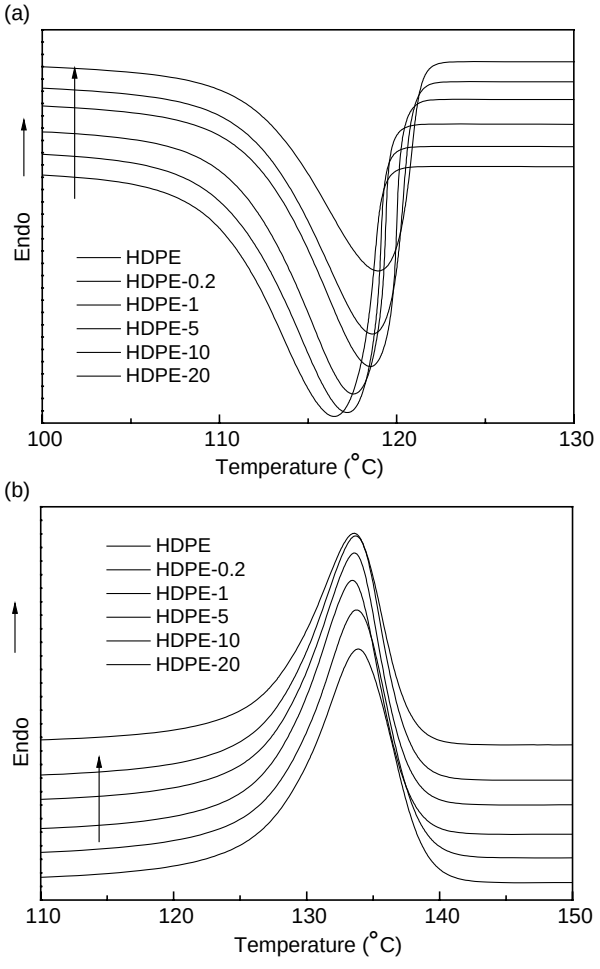

Fig. 3. DSC (a) cooling and (b) heating scan thermograms of HDPE and HDPE/silicalite-1 nanocomposites.

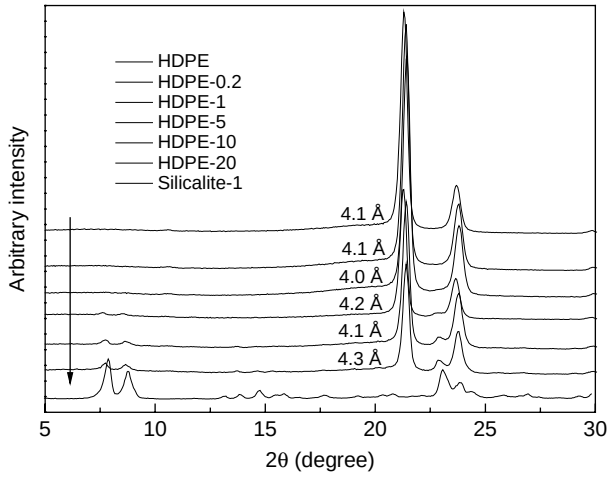

Fig. 5. WAXD patterns of HDPE and HDPE/silicalite-1 nanocomposites. The apparent crystal sizes of (110) reflections of HDPE are indicated in the figure.

silicalite-1 in the sample surface significantly decreases above a critical loading level as much as decreasing the peak intensity of the polymer. In addition, to evaluate the effect of silicalite-1 on the crystal size of HDPE the apparent crystal sizes (L_{hkl}) of (110) reflections of HDPE, which do not overlap in the scattering angle with those of silicalite-1, are calculated using the following Scherrer equation

$$L_{hkl} = \frac{K\lambda}{\beta \cos\theta} \quad (1)$$

where β is the half-width of the diffraction peak, θ the Bragg angle, K the correction factor ($K=0.9$), λ the wave length of the X-ray beam ($\lambda=0.1542$ nm). The apparent crystal sizes of HDPE are little affected by the presence of silicalite-1 ranging 4.0–4.3 Å resulting in little difference in the melting temperature. This suggests that the HDPE/silicalite-1 nanocomposites exhibit a two-phase structure consisting of polymer and nanoparticle.

Fig. 6 shows dynamic viscosity (η') curves of HDPE and HDPE/silicalite-1 nanocomposites at 150 °C, a typical pattern of pseudoplastic polymer. Newtonian behavior is observed in the low frequency range after which shear thinning is followed. The incorporation of nanoparticles increases the η' of HDPE with silicalite-1 content. This suggests that silicalite-1 nanoparticles limit the mobility of polymer chain near the nanoparticles. In other words, the contact probability between nanoparticle and polymer chain is increased with silicalite-1 content leading to an increased friction as much as increasing η'. In particular, the HDPE nanocomposites with silicalite-1 more than 10 wt% show yield behavior. This indicates that a significant increase in heterogeneity in the system starts from 10 wt%. In addition, the difference of η' between HDPE and its nanocomposites becomes small with increasing the frequency. This implies that the confinement of polymer chains near the nanoparticle is not much in the relatively high frequency range.

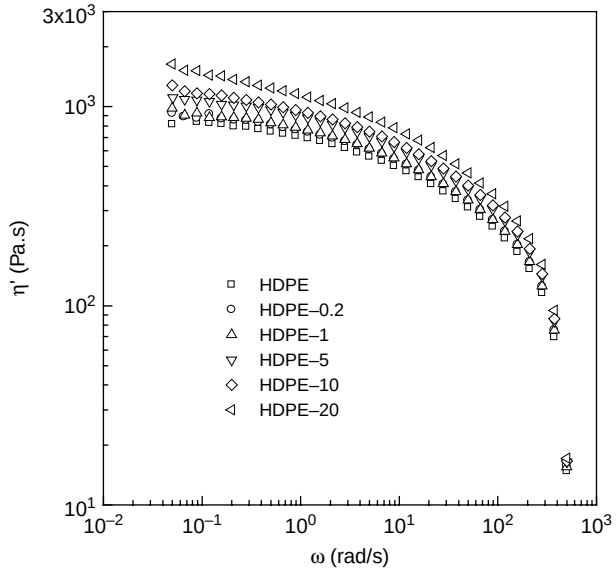

Fig. 6. η' curve of HDPE and HDPE/silicalite-1 nanocomposites at 150°C.

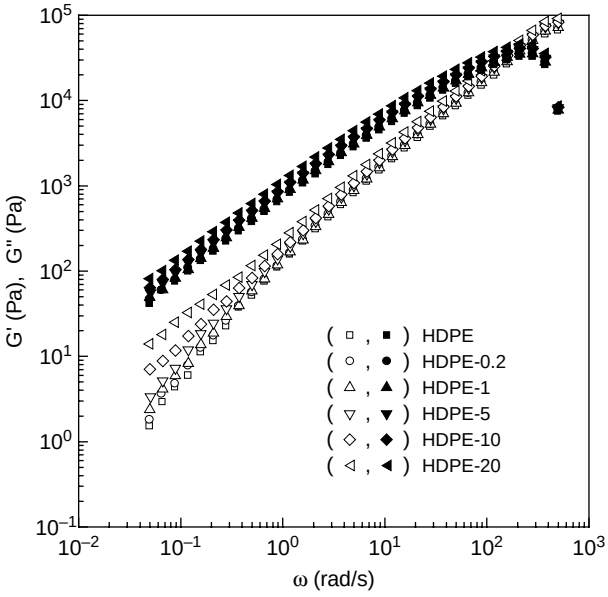

Fig. 7. Dynamic modulus curve of HDPE and HDPE/silicalite-1 nanocomposites at 150 °C.

The storage modulus (G') and loss modulus (G'') of HDPE and HDPE/silicalite-1 nanocomposites are plotted against frequency in Fig. 7. The presence of the nanoparticles increases both G' and G''. In particular, introducing the nanoparticles has a more noticeable effect on the G' than on G'' in the low frequency range. The nanocomposites with slilicalite-1 more than 10 wt% show the inflection points for G'. After the points, the difference of G' between HDPE and its nanocomposites becomes small. This phenomenon can be inferred that the increase of solid-like properties of the polymeric system is notable if the frequency is enough low for the particle to restrict the mobility of polymer chain.

Fig. 8 shows logarithmic plot of G' versus G'' at 150 °C, the so-called, cole–cole plot. Introducing silicalite-1 up to 5 wt% gives a single master curve whose slope is 1.37, while further addition exhibits the inflection in the low frequency range. HDPE-10 and HDPE-20 give the slope 1.22 and 1.02, respectively, prior to the inflection points, after which the slope increases up to that of pure HDPE. Theoretically, the slope of 2 is frequently encountered with isotropic and homogeneous polymer solutions without any specific interaction. Reduced slope prior to the inflection point reflects the formation of an increased heterogeneity by the interference of silicalite-1 nanoparticle in the chain mobility. That is, much energy would be dissipated by collapsing the heterogeneous structures resulting in the increase of the slopes. However, there is little scattering of data points from of the master curve in the high frequency range. This clarifies that the presence of nanoparticles does not affect the conformation of polymer chain because little adsorption of the polymer chains on the surface of the nanoparticles may also take place as previously mentioned.

It is recognized that yield behavior of heterogeneous systems is well characterized by adopting the Casson plot

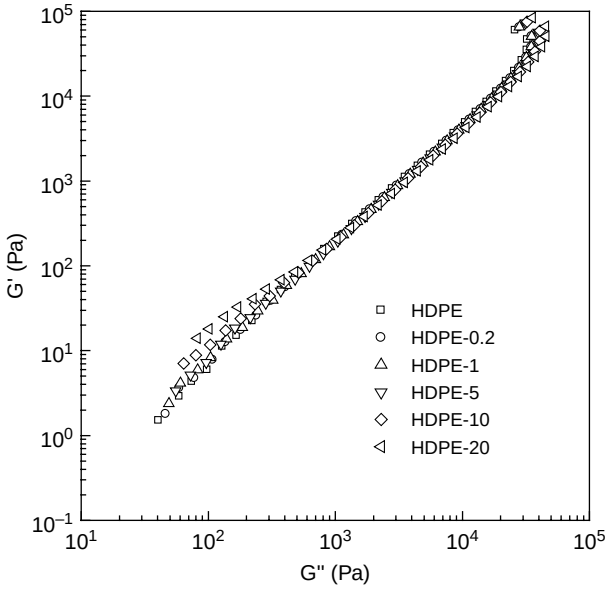

Fig. 8. Logarithmic plot of G' versus G'' of HDPE and HDPE/silicalite-1 nanocomposites.

defined by

$$G''^{1/2} = G''^{1/2}_{y} + K\omega^{1/2} \quad (2)$$

in which G''_{y} stands for yield stress and K is constant. The Casson plot reveals a non-zero positive intercept for all the samples as presented in Fig. 9. G''_{y} increases with silicalite-1 content. The introduction of silicalite-1 more than 10 wt% gives a significant increase in yield stress, indicative of such a great increase in heterogeneity in the system.

The presence of some pseudostructure caused by the presence of nanoparticles affects the relaxation behavior as well. Characteristic relaxation times (λ) of polymeric materials are calculated using an empirical equation substituted by

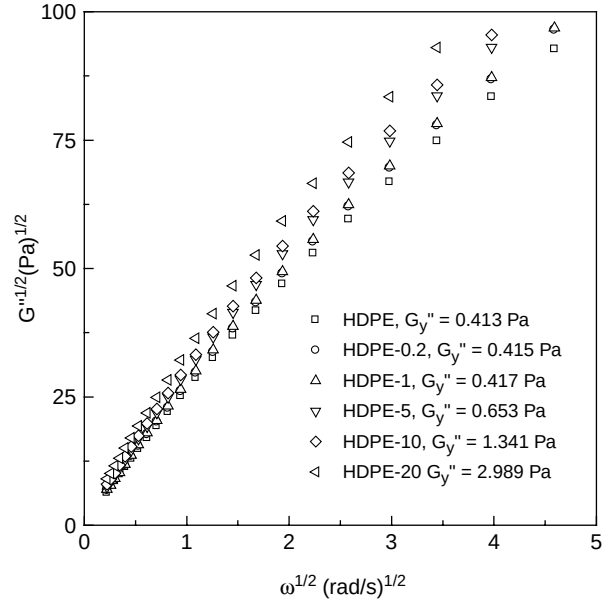

Fig. 9. Casson plot of HDPE and HDPE/silicalite-1 nanocomposites.

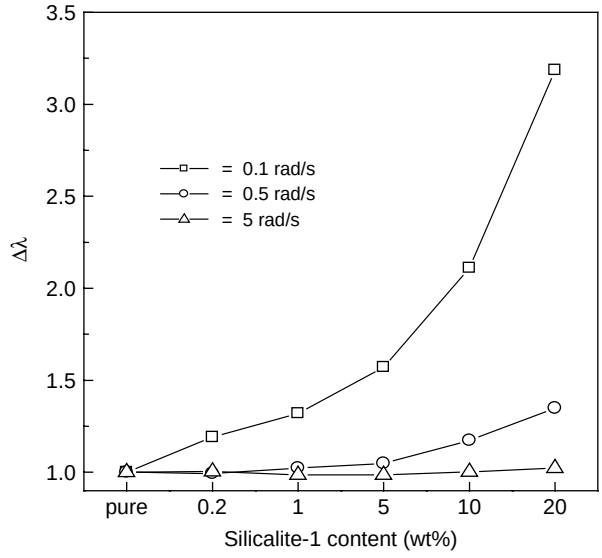

Fig. 10. Variation of $\Delta\lambda$ with silicalite-1 content at several frequencies.

dynamic rheological parameters,

$$\lambda = \frac{G'}{(|\eta^*| \times \omega^2)} \quad (3)$$

where η^* is the complex viscosity. If there is some molecular order or physical structure, much longer relaxation time is expected [15]. To elucidate the effect of the silicalite-1 nanoparticle on the relaxation time at various frequencies, a normalized relaxation time ($\Delta\lambda$) is defined by ratio of λ of the nanocomposite to that of pure HDPE at the corresponding frequency. Fig. 10 shows the variation of $\Delta\lambda$ with silicalite-1 content at three different frequencies. The increasing influence of the nanoparticles on $\Delta\lambda$ is much greater at higher silica content and at lower frequency. In the presence of silicalite-1 nanoparticles HDPE chain is constrained owing to the narrow space surrounded by the dispersed nanoparticle resulting in long relaxation times. In addition, little difference of $\Delta\lambda$ at a high frequency of 5 rad/s implies that the influence of shearing on the mobility of polymer chain is superior to that of the nanoparticles in this system where little interaction exists between nanoparticle and polymer.

A plot of storage modulus (G') versus time at a given isothermal crystallization temperature is shown in Fig. 11. From rheological principles, the isothermal dynamic crystallization behavior may be assessed by following the variation of G' with time at a given temperature. In this plot, G initially increases monotonically with time before the nuclei become crystallites of a critical size under shear. This period is referred to as the induction time for crystallization. As the crystallites grow to larger sized spherulites within the system through nucleation and growth, the homogeneous melt system changes into the heterogeneous system [16]. This may be responsible for abrupt increase of G'. Then a level-off of G' with time reveals that the system reaches an equilibrium. The ceiling value of G' is little affected by frequency, temperature, and the loading level. The crystallization time is determined by the

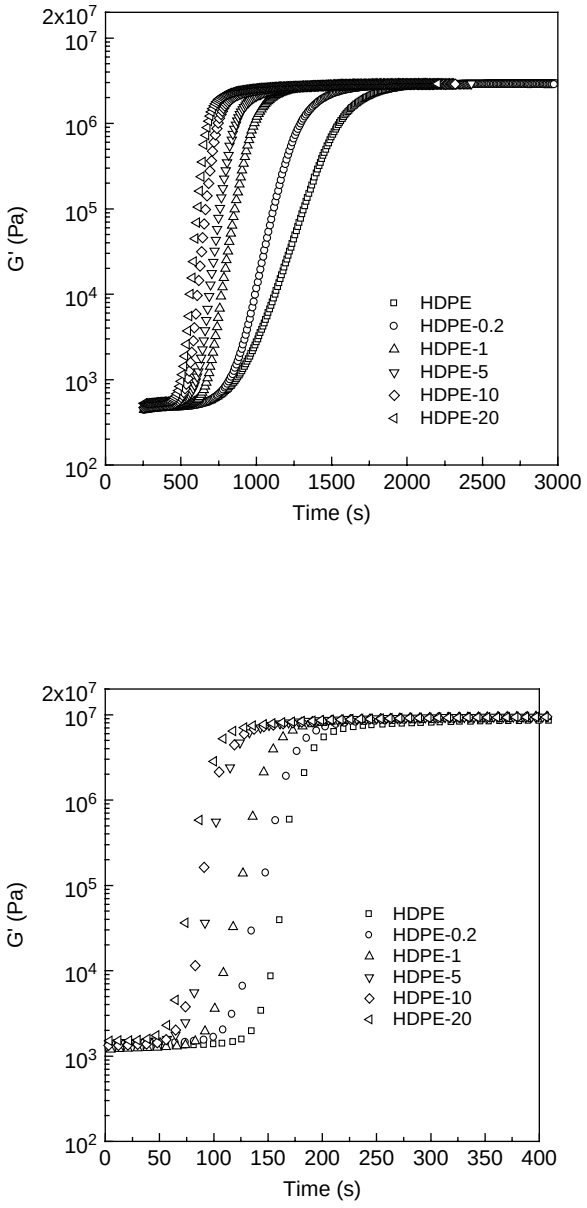

Fig. 11. Variation of G' with time at 5 rad/s at an isothermal crystallization temperature of (a) 125 and (b) 120 °C.

difference between the onset time of crystallization when the abrupt increase of G' starts and the final time when G' levels off. In addition, the G' versus time data can be normalized to give a relative crystallinity function of time, from which the half-time for crystallization ($t_{1/2}$) is determined. The induction time, crystallization time, and half-time of crystallization ($t_{1/2}$) are summarized in Table 1. The introduction of silicalite-1 nanoparticle accelerates the overall crystallization process of HDPE. Further, the promotion effect of silicalite-1 on the crystallization behavior is more notable at 125 °C than at 120 °C. The silicalite-1 content more than 5 wt% has little effect on the crystallization time and $t_{1/2}$ but decreases the induction time at 120 °C. The rate of crystallization of polymers is determined from a concurrent nucleation and growth processes. Growth rate is dominant factor in determining the crystallization rate at relatively low temperature. The nanoparticles hinder the participation of polymer chain in crystallizable unit by reducing the chain mobility as well as act as a nucleation agent. Thus, the role of the nanoparticles becomes counterbalanced in the high silicalite-1 content more than 5 wt% at relatively low crystallization temperature, 120 °C. On the contrary, at relatively high crystallization temperature where little nucleation and high mobility of polymer chain are guaranteed, the role of the nanoparticle as a nucleating agent is more effective leading to a decreased induction time and crystallization time with increasing silicalite-1 content.

Table 1
Induction time, crystallization time and half-time of crystallization ($t_{1/2}$) data, determined from the G' versus time curves

Freqency and temperature	Sample	Induction time (s)	Crystallization time (s)	$t_{1/2}$ (s)
125 °C, 5 rad/s	HDPE	389	1420	975
	HDPE-0.2	374	1124	725
	HDPE-1	286	866	493
	HDPE-5	248	792	403
	HDPE-10	200	639	318
	HDPE-20	163	619	287
120 °C, 5 rad/s	HDPE	103	219	91
	HDPE-0.2	87	184	94
	HDPE-1	70	169	88
	HDPE-5	55	164	68
	HDPE-10	47	166	71
	HDPE-20	38	158	68

4. Conclusions

The silicalite-1 nanoparticles played a role of nucleating agent for HDPE and thereby promoted crystallization through heterogeneous nucleation. They also improved the thermal stability showing that the onset point of degradation shifted to higher temperature. However, the presence of the nanoparticles has little effect on the crystalline morphology of HDPE within the loading level observed.

The introduction of silicalite-1 nanoparticles, particularly, more than 10 wt% increased the η' and G' of HDPE in the low frequency range. This was attributed to the fact that the nanoparticles limit the chain mobility by surrounding it. However, there was little change in viscoelastic properties relatively in the high frequency range irrespective of the presence of silicalite-1. This suggested that there existed weak interaction between HDPE and siliclalite-1 and that the constraint of the chain mobility by the nanoparticles could be collapsed by applying high shear rate. The HDPE nanocomposites showed the promoted dynamic crystallization behavior with increasing silicalite-1 content. In particular, the nucleation activity of the nanoparticle was high at relatively high temperature leading to decreased induction time as well as crystallization time.

References

[1] Bartczak Z, Argon AS, Cohen RE, Weinberg M. Polymer 1999;40: 2347–65.
[2] Ke Y, Long C, Qi Z. J Appl Polym Sci 1999;71:1139–46.
[3] Yano K, Usuki A, Okada A. J Polym Sci, Part A: Polym Chem 1997;35: 2289–94.
[4] Pawlak A, Zinck P, Galeski A, Gerard JF. Macromol Symp 2001;169: 197–210.
[5] Rong JF, Jing ZH, Li HQ, Sheng M. Macromol Rapid Commun 2001;22: 329–34.
[6] Giannelis EP. Adv Mater 1996;8:29–35.
[7] Kurauchi T, Okada A, Noumra T, Nishio T, Saegusa S, Deguchi R. Soc Automot Eng Techical Paper, Series No 910584; 1991.
[8] Kalipcilar H, Culfaz A. Cryst Res Technol 2000;35:933–42.
[9] Vaia RA, Ishii H, Giannelis EP. Chem Mater 1993;5:1694–6.
[10] Christiani BR, Maxfield M. US Patent 5747560; 1998.
[11] Safadi B, Andrews R, Grulke EA. J Appl Polym Sci 2002;84:2660–9.
[12] Yang F, Ou Y, Yu Z. J Appl Polym Sci 1998;69:355–61.
[13] Weimer MW, Chen H, Giannelis EP, Sogah DY. J Am Chem Soc 1999; 121:1615–6.
[14] Liu L, Qi Z, Zhu X. J Appl Polym Sci 1999;71:1133–8.
[15] Wissburn KF, Griffin AC. J Polym Sci, Polym Phys Ed 1982;20:1835–45.
[16] Yoon WJ, Myung HS, Kim BC, Im SS. Polymer 2000;41:4933–42.